3.1.5. SPECIAL STUDIES

Comparison of Aerosol Light Scattering and Absorption Measurements

CMDL has measured both aerosol light scattering (since 1976) and aerosol light absorption (since 1988) at BRW. To obtain data representative of clean baseline conditions, measurements from the polluted sector, defined by wind speed and direction, are automatically removed from the data set. Table 3.5 lists the instruments and their period of operation at Barrow. Initially, light scattering was measured using a 4-wavelength nephelometer, and light absorption was measured using an aethalometer. This original sampling system did not include size or relative humidity control of the aerosol sample. New light scattering and absorption instruments were installed at BRW (within 2 meters of the old instruments) in October 1997. The new instruments are designated for North Slope, Alaska (NSA) to distinguish them from the co-located BRW instruments. The new system obtains measurements at two size cuts by using a valve to switch between a 10 µm and 1 µm impactor. Relative humidity is maintained at or below 40% by heating the air sample. The BRW and NSA systems were operated simultaneously for approximately 1 year (fall 1997–fall 1998). One year of simultaneous light scattering measurements and 2 years of light absorption measurements from the co-located instruments were compared. It is important to understand how measurements from these instruments compare in order to maintain data consistency for the entire measurement period.

The comparison procedure was:
- Select data for the overlap period October 1997 to October 1998 for σ_{sp}, and October 1997 to October 1999 for σ_{ap}
- Estimate the absorption coefficient for the aethalometer using: $\sigma_{ap} = 10 \text{ m}^2/\text{g} * [BC]$
- Apply quality control edit corrections to data sets (e.g., remove spikes and contaminated data)
- For the NSA data set, use only 10 µm size cut data
- Correct the NSA particle soot absorption photometer (PSAP) data for: (a) scattering by particles within the filter and (b) spot size. Also, remove low transmittance data (e.g., transmittance <0.5 as per *Bond et al*. [1999])

- Calculate hourly averages of scattering and absorption coefficients
- Calculate daily averages of absorption for the aethalometer and PSAP
- Remove obvious outliers (four points for the σ_{ap} data)
- Determine the least squares linear fit and correlation coefficient for the data sets. Perform the regression for both a calculated and forced-to-zero y-intercept

Figure 3.5 shows that, for the 2 years, there is a relatively low correlation between the hourly averaged PSAP and aethalometer measurements ($R^2 = 0.70$), although the instruments agree fairly well (the slope is 0.94). Looking at the data on a year-by-year basis, the two instruments demonstrated better agreement with each other for the second-year period than for the first year (slope = 0. 99, $R^2 = 0.77$ and slope = 0.92, $R^2 = 0.66$, respectively). This difference is statistically significant, but it is unclear what caused this difference.
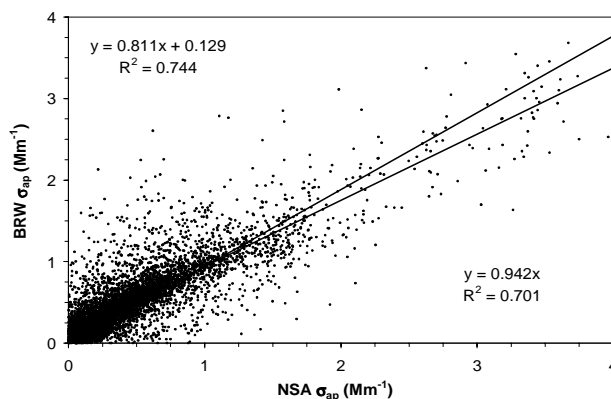

Fig. 3.5. Comparison of hourly averaged absorption data from NSA and BRW, October 1997-October 1999.

TABLE 3.5. Description of Instrumentation at Barrow, Alaska

Instrument	Period of Operation	Station	Comments
MRI nephelometer	1976-fall 1998	BRW	4 wavelength, no size cut
Magee Scientific aethalometer	1988-present	BRW	Broadband, no size cut
			Specific absorption of 10 m^2/g used to convert [BC] to σ_{ap}
TSI nephelometer (model no. 3563)	Fall 1997-present	NSA	3 wavelength, 1 and 10 µm size cut
Radiance Research particle soot absorption photometer (PSAP)	Fall 1997-present	NSA	565 nm wavelength, 1 and 10 µm size cut

For daily averaged data (Figure 3.6) there is a stronger relationship between the two instruments' measurements than for hourly averaged data and, again, good agreement for the two measurements of absorption coefficient. Because particle concentrations and hence, light absorption, are low at the site, often near the detection limits of the two instruments, there is considerable noise in the measurements. The improvement in fit for the daily averaged values with respect to the hourly averaged values is most likely a result of averaging noise in the data over a longer time period.
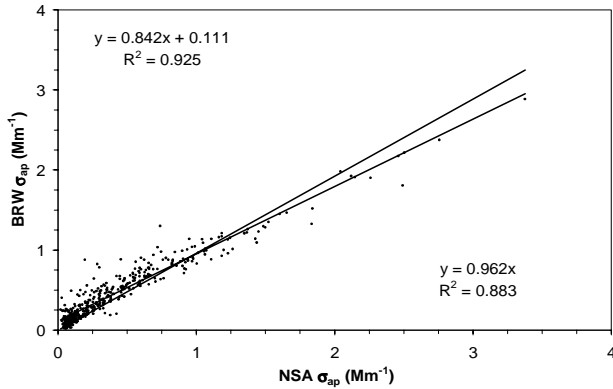

Fig. 3.6.   Comparison of daily averaged absorption data from NSA and BRW, October 1997-October 1999.

Figure 3.7 shows the hourly variability in the ratio of the two instrument measurements as a function of absorption coefficient. The relationship between the two instruments appears less variable at higher absorption coefficients ($\sigma_{ap} > 1$ Mm^{-1}) but only about 10% of the data are in this range. At low absorption values ($\sigma_{ap} < 1$ Mm^{-1}) there is considerable variability due to instrument noise. Interestingly, while the aethalometer data are lower than PSAP data for high absorption coefficients (consistent with the linear fit results), the aethalometer measurements tend to be lower than the PSAP's at low σ_{ap}.
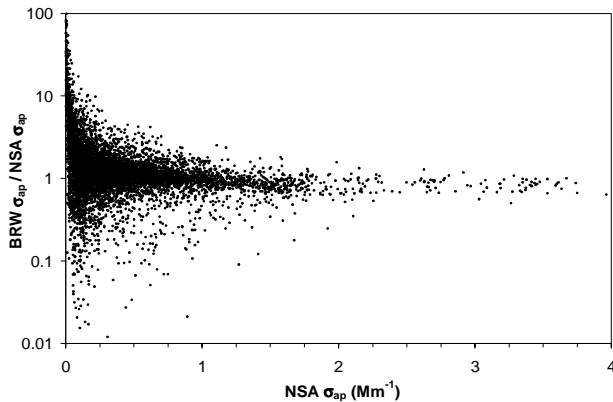

Fig. 3.7.   Variation in the ratio of absorption measured at BRW to that measured at NSA as a function of hourly averaged absorption coefficient.

Table 3.6 summarizes the fit parameters for the absorption coefficient. Overall, the linear fits suggest that the BRW measurements were consistently lower than the NSA measurements. There are other questions that need to be addressed in the future with respect to measurements of σ_{ap} at Barrow. These include: How much do the differences in wavelength of the two instruments influence σ_{ap}? Are there corrections that should be applied to the aethalometer: for example some sort of spot size correction? How appropriate is the arbitrarily chosen 10 m^2/g used to convert from mass concentrations measured by the aethalometer into scattering coefficients?

TABLE 3.6.   Results From Linear Fits of Data to Equation: BRW = m*NSA for Absorption Coefficient

Parameter	Slope (m)	R^2	Number of Points
σ_{ap} (hourly) year 1	0.92 ± 0.01	0.66 ± 0.01	3456
σ_{ap} (hourly) year 2	0.99 ± 0.01	0.77 ± 0.01	3562
σ_{ap} (hourly) both years	0.94 ± 0.01	0.70 ± 0.01	7018
σ_{ap} (daily) year 1	0.94 ± 0.03	0.88 ± 0.02	223
σ_{ap} (daily) year 2	1.03 ± 0.03	0.87 ± 0.02	226
σ_{ap} (daily) both years	0.96 ± 0.02	0.89 ± 0.01	449

In addition to comparing absorption coefficient measurements, comparisons of scattering coefficient as a function of wavelength for the BRW and NSA nephelometers were also made for 1 year starting October 1997 (Table 3.7). For the two nephelometers there is high correlation despite low particle concentrations and hence low scattering measurements. The blue scattering coefficients (σ_{spB}) have the weakest agreement (slope = 0.92). This may be because of problems with the blue photomultiplier in the BRW nephelometer. The blue scattering measurement at BRW was often similar to or even lower than the green scattering measurement, while at NSA the $\sigma_{spB}/\sigma_{spG}$ ratio was typically greater than 1 as expected.

TABLE 3.7.   Results From Linear Fits of Data to Equation: BRW = m*NSA for Scattering Coefficient

Parameter	Slope (m)	R^2	Number of Points
σ_{spB}	0.92 ± 0.00	0.95 ± 0.01	3456
σ_{spG}	1.00 ± 0.00	0.94 ± 0.01	3456
σ_{spR}	0.97 ± 0.00	0.94 ± 0.01	3456

Differences between the two instruments may be attributable to several factors. Optically, the two nephelometers are (almost) identical, so it was assumed that correcting for the truncation angle would not improve the comparison. Thus for this comparison no corrections for truncation were applied to either instrument. Changes in filter bandpass and calibration error may also play a role.

Optical Property of Indian Ocean Aerosols

During February and March 1999 the CMDL aerosol group participated in the Indian Ocean Experiment (INDOEX), a multi-platform field campaign that took place over the Indian Ocean. A central focus of the campaign was to assess the role of aerosols from the Indian subcontinent on direct and indirect radiative forcing, as well as the role of convective cirrus in aerosol transport and photochemical processing.

This region of the world has a fast growing population that is becoming more industrialized with emissions of CO_2, aerosols, and sulfates expected soon to surpass those of North America and Europe. Because of these potentially high future emissions, an understanding of climate forcing and transport of trace gases and aerosols in this region is critical to being able to predict global climate forcing.

The INDOEX campaign was based at the Maldive Islands, about 700 km southwest of India. As part of the campaign, CMDL performed in situ measurements of aerosol optical properties on two separate platforms: the Scripps Institution of Oceanography (SIO) climate observatory on the island of Kaashidhoo (KCO) and onboard the NCAR C-130 aircraft. These measurements included the aerosol total and hemispheric backscattering coefficients, the aerosol hygroscopic growth factor (f(RH)), and the aerosol absorption coefficient. Here the aerosol hygroscopic growth factor is defined to be the ratio of the aerosol scattering coefficient at 85% relative humidity to the aerosol scattering coefficient at 40% relative humidity.

During the northeast monsoon season (January-April) the Intertropical Convergence Zone is south of the island and air circulation is from the Indian subcontinent. Thus aerosols measured at KCO during this time represent polluted continental air masses. Figure 3.8 shows a time series of the measured aerosol optical properties at KCO.

Back trajectory calculations show a change in the air mass origin on March 7 (Day 66) from the east Bay of Bengal region to the west Arabian Sea. Evidence of this change is apparent in a decreased aerosol loading and accompanied by lower σ_{sp} and σ_{ap} values. Despite this difference in aerosol loading, the aerosol intensive properties of single-scattering albedo, backscatter fraction, and hygroscopic growth are similar between the two regions. The lower aerosol loading in the Arabian Sea air masses likely resulted in a larger contribution to the total scattering from supermicron seasalt particles as evident in the smaller fractions of submicron aerosol scattering and absorption from the Arabian Sea.
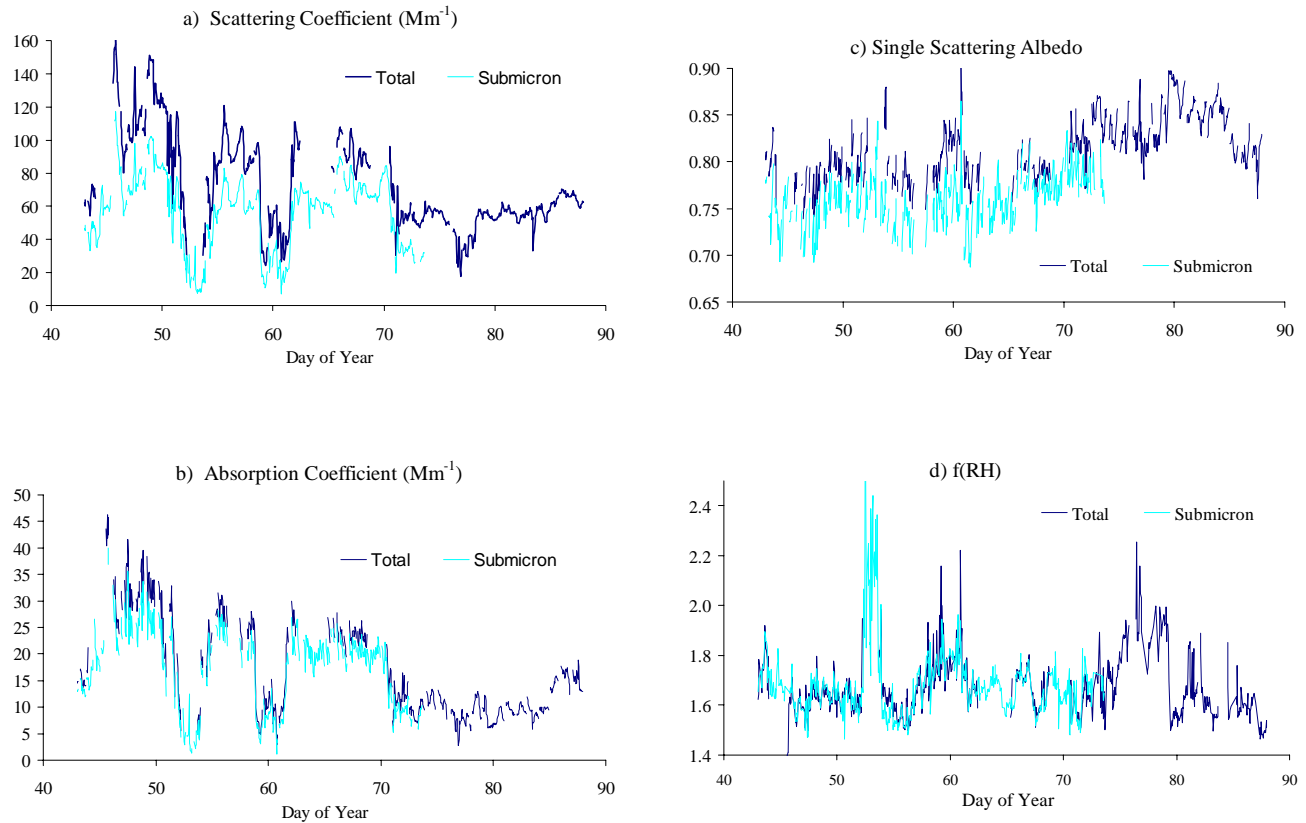

Fig. 3.8.   Time series of measurements from KCO in 1999: (a) aerosol total and submicron scattering coefficient, (b) aerosol total and submicron absorption coefficient, (c) aerosol total and submicron single scattering albedo, (d) aerosol total and submicron hygroscopic growth. All values are reported for 550 nm wavelengths.

In addition to surface-based measurements at KCO, aerosol optical properties were measured in situ from the NCAR C-130 research aircraft using an aircraft version of the ground-based CMDL aerosol measurement system. Aircraft measurements were necessary for information on spatial (i.e., horizontal and vertical) and temporal variability of aerosol optical properties. Vertical profiles and horizontal legs at altitude were conducted to characterize aerosol variability in the region with coverage of much of the Indian Ocean Basin between 8°S and 17°N.

The measured aerosol light scattering coefficients over the northern Indian Ocean were typically several times those observed at perturbed continental sites in the United States. The highest aerosol concentrations were observed in the northern Indian Ocean (north of the Maldives). The aerosol was substantially darker than U.S. sites with an average single-scattering albedo for all flights near 0.85. The optical depths in the region, calculated using aircraft aerosol optical property data, were in the 0.15-0.35 range for most days. Elevated aerosol layers, decoupled from the surface, were observed in over one-third of the vertical profiles. Figure 3.9 shows two vertical profiles, with one profile showing an elevated aerosol layer.
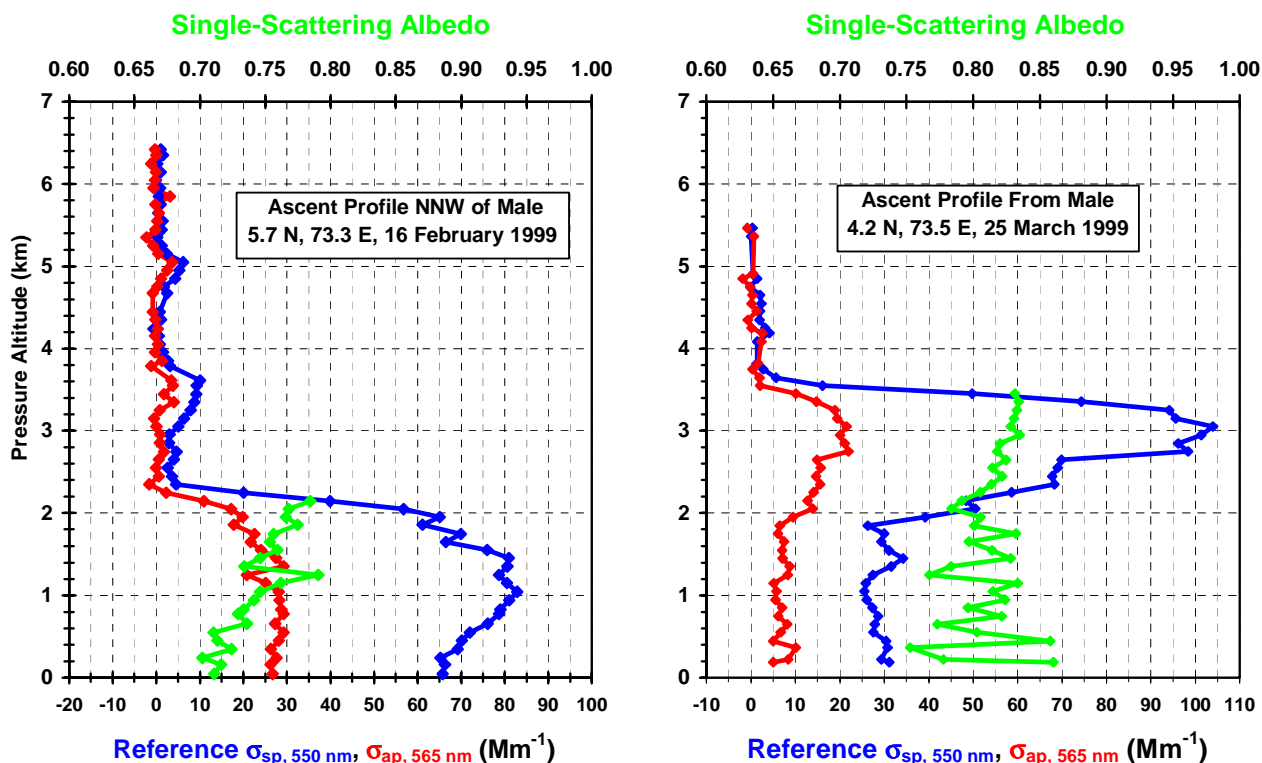

Fig. 3.9. Two vertical profiles of total scattering coefficient (σ_{sp}, red), absorption coefficient (σ_{ap}, blue), and single-scattering albedo (green) obtained by CMDL instruments onboard the NCAR C-130 aircraft. The profile on the left shows a thick aerosol layer from the surface to ~2 km. The profile on the right shows an elevated aerosol layer with a peak at ~3 km altitude.

Table 3.8 lists the mean values of the measured parameters and compares them to those from other CMDL surface sites. In comparison to aerosol properties measured at Bondville (a U.S. continental site) and Sable Island (a Canadian marine site) the aerosol from the Indian subcontinent has a far greater absorption coefficient. Unlike aerosols from U.S. continental sites, the single scattering albedo at KCO declines with an increase in aerosol loading (Figure 3.10). Apparently under highly polluted conditions the aerosol soot fraction relative to sulfate is higher than that from U.S. sites. This difference could reflect the regional sources of sulfate and carbon as well as rates of in-cloud sulfate oxidation. Although the Indian subcontinent aerosol has a large absorbing fraction, its mean hygroscopic growth is similar to that from regions with less absorbing aerosol. This difference points to either a significantly different composition or morphology for the absorbing components of aerosols from the Indian subcontinent with respect to North America.

TABLE 3.8. Means and Variabilities of Pollution Aerosols

Aerosol Property	Bay of Bengal	Arabian Sea	Sable Island	Bondville
σ_{sp}	95 ± 20	54 ± 9	42 ± 35	60 ± 49
σ_{ap}	25 ± 7	10 ± 3	2 ± 2	5 ± 4
$F\sigma_{sp}$	0.70 ± 0.06	0.62 ± 0.05	0.26 ± 0.10	0.86 ± 0.07
$F\sigma_{ap}$	0.85 ± 0.04	0.80 ± 0.07	0.81 ± 0.10	0.82 ± 0.10
f(RH)	1.65 ± 0.10	1.67 ± 0.14	1.7 ± 2.7[*]	1.5 ± 0.4[†]

[*]*McInnes et al.* [1998]

[†]S. Koloutsou-Vakakis, et al., Aerosol properties at a midlatitude northern hemisphere continental site, submitted to *J. Geophys. Res.*, 1999

Scattering coefficients, σ_{sp}, are measured at $\lambda = 550$ nm. Absorption coefficients are measured at $\lambda = 565$ nm. $F\sigma_{sp}$ and $F\sigma_{ap}$ are the submicron fractions of aerosol scattering and absorption, respectively. f(RH) is given for a relative humidity of 85% relative to 40%. Variabilities are reported as ± 1 standard deviation. Sable Island, Nova Scotia, and Bondville, Illinois, are anthropogenically perturbed marine and continental sites, respectively. The range of f(RH) at Sable Island is between polluted and clean air masses observed over a ~10-day period. Time periods of 4 hours before and after rain events were excluded from the KCO data.
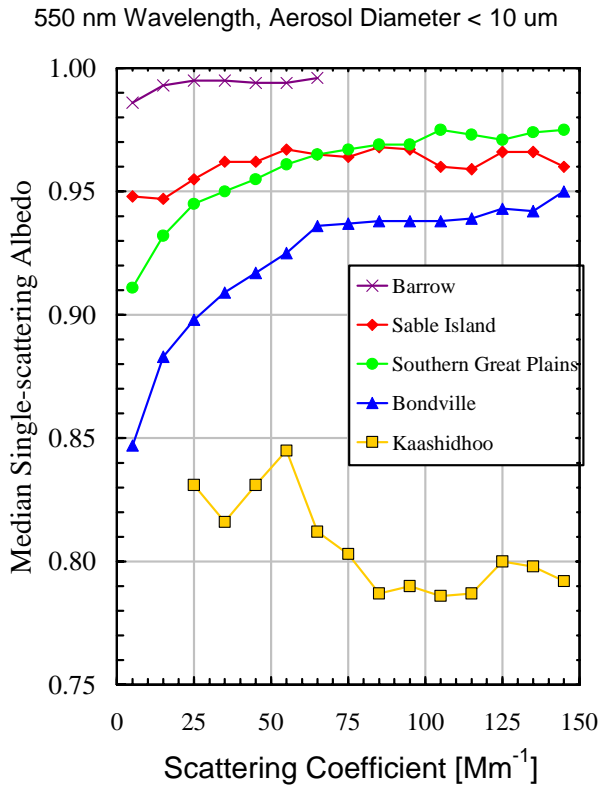

Fig. 3.10. Aerosol single-scattering albedo plotted against scattering coefficient (hourly average data). Data are from the four CMDL North American monitoring stations (entire period of record) and the Kaashidhoo Island station in the Indian Ocean (February and March 1999).